Research Square

Preprints are preliminary reports that have not undergone peer review.
They should not be considered conclusive, used to inform clinical practice,
or referenced by the media as validated information.

Preparation and Performance Evaluation of Degradable IPN-PAM/STA Interpenetrating Network Microspheres for In-Depth Profile Control

Guangliang Jia
China University of Geosciences Faculty of Engineering
Guiru Liu
Xi'an Rare Metal Materials Institute Co., Ltd. Xi'an
Daoming Zheng
Sinopec North China Petroleum Engineering Co
Yunchao Cheng
Sinopec North China Petroleum Engineering Co
Xin Wen
3671854115@qq.com

Shaanxi University of Science &Technology

Research Article

Keywords: Microspheres, Reverse emulsion polymerization, Interpenetrating network, Profile control and water shutoff, Biodegradability, Oil reservoir adaptation

Posted Date: August 5th, 2026

DOI: https://doi.org/10.21203/rs.3.rs-10355356/v1

License: This work is licensed under a Creative Commons Attribution 4.0 International License.
Read Full License

Additional Declarations: No competing interests reported.

Preparation and Performance Evaluation of Degradable IPN-PAM/STA Interpenetrating Network Microspheres for In-Depth Profile Control

Guangliang Jia[1,2], Guiru Liu[4], Daoming Zheng[2], Yunchao Cheng[2]，Xin Wen[*3], Xin Wen

E-mail: 3671854115@qq.com

1 China University of Geosciences Faculty of Engineering, Wuhan, 430074, China

2 Sinopec North China Petroleum Engineering Co.,Ltd，Zhengzhou, 450006, China

3 Shaanxi University of Science &Technology, Xi'an, Shaanxi 710021, China

4 Xi'an Rare Metal Materials Institute Co., Ltd. Xi'an, Shaanxi 710021, China

Abstract: Conventional polyacrylamide (PAM) microspheres suffer from rapid uncontrolled swelling, poor temperature/salt resistance, and severe shear fragmentation, which greatly restrict their application in in-depth profile control and water shutoff of complex oil reservoirs. Herein, novel interpenetrating network microspheres (IPN-PAM/STA) were successfully fabricated via reverse emulsion polymerization, using polyacrylamide (PAM) as the primary network and acid-modified starch (STA) as the secondary crosslinking network. Structural characterizations including FTIR, XRD, TGA and DSC verified the successful construction of stable IPN structures, in which the crystalline structure of starch was completely transformed into an amorphous state through hydrogen-bonding interactions with PAM chains. Benefiting from the synergistic dual-network effect, the optimized IPN-PAM/STA microspheres exhibited controllable swelling behavior, excellent thermal stability above 70 °C, and prominent adaptability to variable salinity and pH environments. Core flooding tests demonstrated an ultra-high plugging efficiency of 96.3%, far superior to that of pure PAM microspheres. More importantly, the introduced biodegradable starch component endows the microspheres with an outstanding biodegradation rate of over 90% within 120 days, effectively avoiding secondary environmental pollution. This work provides a high-efficiency, shear-resistant, temperature-salt tolerant and eco-friendly plugging material for

in-depth reservoir profile control, offering a promising strategy for enhanced oil recovery in heterogeneous and complex oilfields.

Keywords: Microspheres; Reverse emulsion polymerization; Interpenetrating network; Profile control and water shutoff; Biodegradability; Oil reservoir adaptation

1. Introduction

Petroleum is an irreplaceable non-renewable natural resource that plays an indispensable role in national economic development, and its proportion in the global energy consumption structure is gradually rising. Nevertheless, the continuous depletion of petroleum reserves has become a bottleneck restricting social progress[1]. Therefore, improving crude oil recovery efficiency and fully utilizing remaining recoverable petroleum resources has become an urgent challenge worldwide. Primary oil recovery relies on natural reservoir energy, which features low investment and simple technical requirements, yet it only achieves an oil recovery factor of merely 10% – 15%. Secondary oil recovery supplements reservoir energy via artificial water injection, which can further raise the recovery factor by only 15% – 20%[2]. Tertiary oil recovery technologies, including thermal flooding, chemical flooding, gas miscible flooding and other approaches, have been widely deployed in major oilfields to exploit deep reservoir formations[3]. With the intensification of oil extraction, reservoirs developed by water injection generally exhibit inherent and acquired formation heterogeneity. Injected water preferentially flows into production wells through high-permeability pore channels[4]. Continuous water scouring further aggravates reservoir heterogeneity in high-permeability zones, forming dominant water flow channels and triggering adverse phenomena such as water coning and water fingering[5]. Excessive water production is an inevitable issue for most waterflooding oilfields in the middle and late development stages. It severely impairs crude oil recovery and brings extra burdens to subsequent oil production operations[6]. Numerous oilfields around the world have entered their middle-late development periods after years of exploitation, accompanied by a continuous rise in water cut of produced fluids[7]. High water cut wastes reservoir energy, reduces the operational

efficiency of pumping equipment, accelerates corrosion and scaling of pipelines and facilities, and increases the cost of surface water treatment. Direct discharge of untreated produced water also causes severe environmental pollution, serving as a primary contributor to unstable oil production and production decline[8]. For low-permeability fractured reservoirs, conventional strategies including adjusting injection-production ratios and oil production intensity barely achieve satisfactory oil increment and water control effects. Accordingly, profile control and flooding technologies are urgently required to enhance oil recovery for heterogeneous reservoirs. Such technologies can retain injected water in reservoirs and convert it into formation driving energy, redirect fluid flow in deep formations, expand swept volume, and ultimately realize effective oil increment and water cut reduction[9]. In recent years, in-depth profile control technology adopts elastic polymer microspheres with nano- and micron-scale particle sizes. After being injected into formations, these microspheres swell upon contact with formation water and block pore throats at appropriate positions, alleviating reservoir heterogeneity and improving oil recovery[10]. Polymer microsphere technology is a novel in-depth profile control and water shutoff technique developed in recent decades. These particulate plugging agents are synthesized via copolymerization of acrylamide monomers and crosslinkers. Their nano/micron particle sizes allow them to penetrate rock pores, and water-swelling performance enables inter-particle bridging to block formation pore throats[11]. Benefiting from small particle size, favorable water dispersibility, deep formation penetration capacity and temperature-responsive swelling behavior, polymer microspheres have been extensively applied for in-depth profile control and water shutoff, greatly boosting oil recovery. Their chemical composition, monomer ratio, microstructure, morphology and particle size distribution jointly determine their application and plugging performances[12-13]. Water-swellable polyacrylamide (PAM) microspheres possess elasticity and deformability, enabling continuous migration and plugging in deep formations for profile control treatment. In the late stage of tertiary oil recovery, fractures and high-permeability channels formed during water flooding lead to severe reservoir heterogeneity, complex pore structures and

high water cut. As a result, the water cut of production wells rises year by year while single-well oil output declines, bringing tremendous difficulties to field production operations. Multiple profile control systems have been developed to tackle this problem, such as bulk swelling particles, microgel particles and PAM microspheres. Among them, PAM microspheres are the most widely applied materials due to their small particle size and excellent plugging performance after swelling. Their wide particle size distribution matches various reservoir conditions, and delayed swelling during deep migration facilitates effective pore plugging. However, widespread field application has exposed obvious drawbacks of conventional PAM microspheres. After water swelling, the enlarged microspheres suffer severe shear fragmentation during underground migration, which drastically weakens their profile control performance year after year. To overcome these deficiencies, this work aims to regulate the swelling rate, enhance mechanical strength, improve temperature and salt tolerance, and strengthen shear resistance of microspheres. Interpenetrating network (IPN) hydrogels are fabricated by constructing the primary network with polyacrylamide and introducing starch as the secondary crosslinking network.

2. Experimental part

2.1. Materials

Acrylamide (AM), Acrylic acid (AA), analytical grade, Shaanxi Runtai Chemical Co., Ltd.; 2-Acrylamido-2-methylpropane sulfonic acid (AMPS), analytical grade, Shouguang Yuyuan Environmental Protection Technology Co., Ltd.; N,N-Methylenebisacrylamide (MBA), analytical grade, Tianjin Damao Chemical Reagent Factory; Sodium hydroxide (NaOH), analytical grade, Tianjin Obokai Chemical Co., Ltd.; Ammonium persulfate (APS), analytical grade, Tianjin Damao Chemical Reagent Factory; Sodium bisulfite (SHS), analytical grade, Tianjin Baishi Chemical Co., Ltd.; Span 80, industrial grade, Shaanxi Changhai Oilfield Additives Co., Ltd.; Nonylphenol ethoxylate-10 (NP-10) and water-soluble starch (STA), analytical grade, Shanghai Macklin Biochemical Co., Ltd.; Phase inversion agent 1307, industrial grade, self-synthesized in laboratory; Azobisisobutyronitrile (AIBN),

analytical grade, Sinopharm Chemical Reagent Co., Ltd.; Sodium chloride (NaCl), Calcium chloride ($CaCl_2$), analytical grade, Tianjin Dingshengxin Chemical Co., Ltd.

2.2 Preparation of PAM/starch interpenetrating network microspheres

Firstly, 80 g white mineral oil, 20 g Span-80 and 10 g NP-10 were blended uniformly to prepare the oil phase, which was then transferred into a 250 mL three-neck flask equipped with a stirrer and a thermometer. In a beaker, 30 g AM and 1.5 g AMPS were dissolved in 20 g deionized water, followed by the addition of 8 g AA and 0.3 g MBA. The mixture was stirred thoroughly on a magnetic stirrer until complete dissolution. Subsequently, 10 g of 20 wt% NaOH aqueous solution was added dropwise slowly, and the system was stirred for 10 min. Afterwards, 5 g of 5 wt% STA aqueous solution was incorporated and stirred for another 10 min to obtain the aqueous phase. The aqueous phase was slowly dropped into the oil phase, and the mixture was stirred at room temperature for 5 min. Nitrogen was purged through the system for 5 min, then 1.5 g of 2 wt% APS aqueous solution was added. After another 10 min of nitrogen purging, 1.5 g of 2 wt% SHS aqueous solution was supplemented, and the polymerization reaction proceeded for 30 min. After the reaction mixture cooled down to room temperature, 5.5 g phase inversion agent was introduced to implement phase inversion. After 10 min of stirring, the emulsion of PAM/STA interpenetrating network microspheres (IPN-PAM/STA) was obtained. The as-prepared IPN-PAM/STA emulsion is shown in Figure 1.

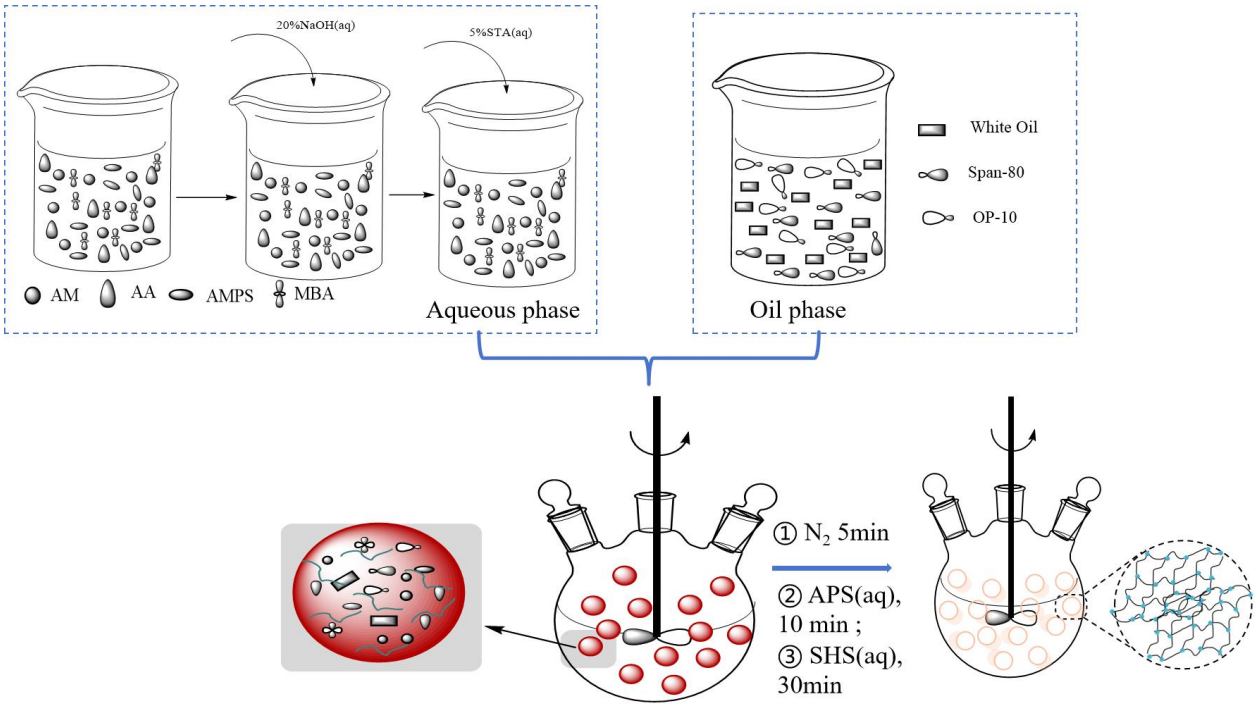


Fig. 1 shows the emulsion synthesis process of interpenetrating network microspheres (IPN-PAM/STA)

2.3 Characterization

2.3.1 Preparation of IPN-PAM/STA Microsphere Powder

The obtained IPN-PAM/STA microsphere emulsion was washed three times with ethanol, followed by freeze-drying at −50 ℃ for 24 h to prepare white powdery IPN-PAM/STA microspheres. 2.3.2 Structural Characterizations of IPN-PAM/STA Microspheres Fourier transform infrared (FTIR) spectroscopy analysis of microsphere powder was performed using a Nicolet iS5 spectrometer (Thermo Fisher Scientific, USA) within the scanning wavenumber range of 4000–400 cm^{-1}. Fully dried and ground microsphere powder was spread and compacted on glass slides, and the crystalline properties of samples were characterized by a D8 Quest X-ray diffractometer (Bruker AXS GmbH, Germany). The synthesized microspheres were prepared into aqueous solutions with a mass fraction of 0.5 %, and their particle sizes were measured via dynamic light scattering (DLS) nanoparticle size and zeta potential analyzer. 2.3.3 TGA Analysis of IPN-PAM/STA Microspheres Thermogravimetric analysis (TGA) was carried out on a TGA Q500 instrument (TA Instruments, USA)

under nitrogen atmosphere. The heating rate was set at 10 ℃/min, and the test temperature ranged from 20 ℃ to 600 ℃ 2.3.4 Salt Resistance Test of IPN-PAM/STA Microspheres At room temperature, NaCl and $CaCl_2$ aqueous solutions with concentrations of 0, 1000, 5000 and 10000 mg/L were adopted as solvents to prepare 0.5 wt% PAM and IPN-PAM/STA microsphere suspensions. A laser particle size analyzer was used to monitor particle size variations of microspheres after swelling for different durations in saline solutions with different mineralization degrees. 2.3.5 Test for pH Effect on Swelling Behavior of IPN-PAM/STA Microspheres Deionized water was replaced by aqueous solutions with pH values of 4, 6, 8 and 9. The particle sizes of IPN-PAM/STA microspheres were measured after 6 h of swelling in each pH environment. 1.5 mol/L HCl and 2.0 mol/L NaOH solutions were used to adjust the pH of acidic and alkaline systems, respectively. 2.3.6 Test for Temperature Effect on Swelling Behavior of IPN-PAM/STA Microspheres IPN-PAM/STA microspheres were immersed in deionized water at 30 ℃, 50 ℃, 60 ℃, 70 ℃ and 80 ℃ for 6 h to determine their particle sizes under different temperature conditions. 2.3.7 Biodegradability Test Samples were dried to constant weight in an oven at 105 ℃, and the initial mass was recorded as m_1. Subsequently, the dried samples were buried in garden topsoil with a soil solution pH of 6 at a depth of 20 cm. After 4 months of soil burial, the samples were retrieved, rinsed with methanol, and dried again to constant weight to obtain the residual mass m_2 [14].

$$\text{Biodegradation rate of samples} = \frac{m_1 - m_2}{m_1} \times 100\%$$

3 Results and Discussion

3.1 Structural Analysis of IPN-PAM/STA

Figure 2(a) shows the infrared spectra of PAM and IPN-PAM/STA. The two spectral lines are largely similar, with significant differences only at 3431 cm^{-1} and 3311 cm^{-1}. This discrepancy arises because these wavelengths correspond to the absorption peaks of O-H and N-H vibrations in the polymer; since starch is the constituent material of the IPN interpenetrated network microspheres and contains numerous O-H bonds, a prominent peak is observed at 3411 cm^{-1}. At

other wavelengths, the spectra are nearly identical: 2921 cm^{-1} and 2850 cm^{-1} correspond to C-H bonds, 1676 cm^{-1} and 1598 cm^{-1} to C=O bonds, while 1442 cm^{-1} and 1371 cm^{-1} represent bending vibration peaks of C-H bonds. These results further demonstrate that acid-treated starch has penetrated into the microsphere interior and formed a network entanglement with the polymer.

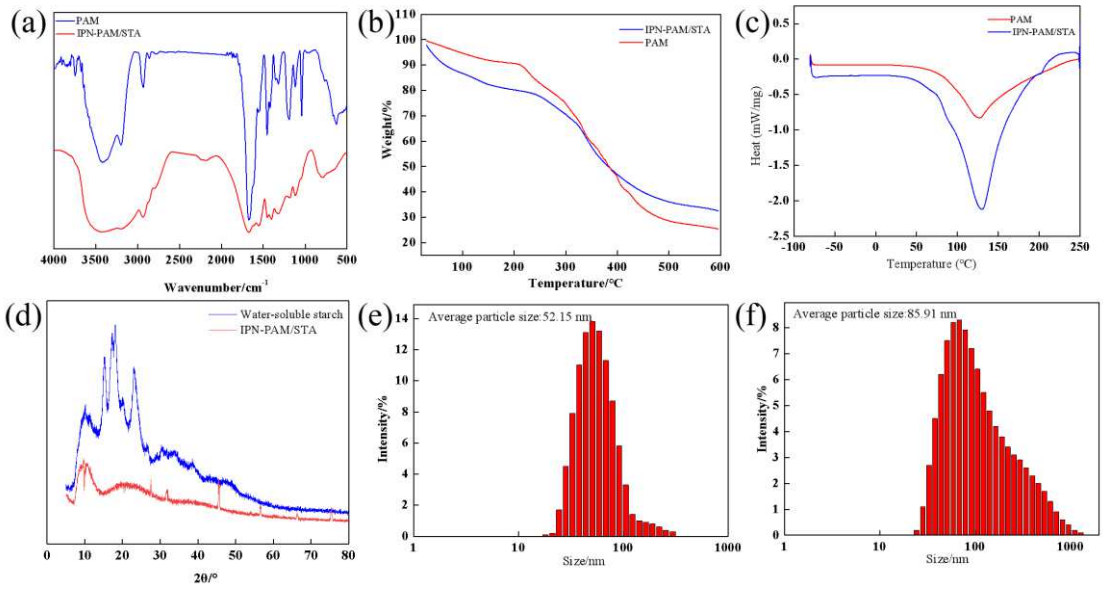


Fig. 2 (a) FTIR spectra of PAM and IPN-PAM/STA, (b) TGA curves of PAM and IPN-PAM/STA, (c) DSC curves of PAM and IPN-PAM/STA, (d) XRD patterns of PAM and IPN-PAM/STA, (e) particle size distribution diagram of PAM, (f) particle size distribution diagram of IPN-PAM/STA

Thermal stability testing is of great significance for evaluating the performance of microspheres. Thermogravimetric tests were carried out on two types of microspheres, and the results are shown in Figure 2(b). It can be observed from the figure that both IPN-PAM/STA and PAM exhibit mass loss below 100 ℃, which originates from the water contained inside the two materials. A comparison of the two spectral curves reveals that the mass loss rate of IPN-PAM/STA is markedly higher than that of PAM. This is because the starch molecular chains in IPN-PAM/STA are rich in hydroxyl groups (-OH), which can form stronger hydrogen-bond networks with water molecules and thus bind more water. Additionally, nanoscale cavities formed by the interpenetrating network structure can physically trap more free water. When the temperature exceeds 400 ℃, the mass loss rate of PAM surpasses that of IPN-PAM/STA, as the interpenetrating network structure retards the depolymerization

of PAM molecular chains via physical crosslinking. These findings demonstrate that IPN-PAM/STA possesses far superior thermal stability compared with conventional microspheres, rendering IPN-PAM/STA microspheres more suitable for oil reservoirs under high-temperature conditions.

Figure 2(c) presents the DSC test results of IPN-PAM/STA and PAM. As illustrated, mass loss gradually occurs within the temperature range of 0 to 100 ℃, which can be attributed to incomplete drying of the samples. A sharp and intense endothermic peak emerges for IPN-PAM/STA at approximately 125 ℃ This phenomenon stems from the starch contained in IPN-PAM/STA microspheres; starch undergoes phase transformation between 120 ℃ and 130 ℃ and converts into yellow dextrin. PAM microspheres display an identical peak at the same temperature, yet with a smaller peak area, which arises from the decomposition of bound water or emulsifier molecules.

Figure 2(d) shows the XRD patterns of IPN-PAM/STA and water-soluble starch. As seen from the patterns, water-soluble starch exhibits strong diffraction peaks at 2θ values of 10°, 15°, 17°, 18°, and 23°, with connected peaks at 17° and 18°, which are characteristic typical diffraction peaks of starch. In contrast, no corresponding peaks appear at the identical positions for IPN-PAM/STA microspheres. The primary reason is that polyacrylamide (PAM) molecular chains and starch (STA) form a molecular-level composite through the interpenetrating network structure. The amide groups (-$CONH_2$) of PAM form strong hydrogen bonds with the hydroxyl groups (-OH) of starch, disrupting the original crystalline regions of starch. Meanwhile, the steric hindrance effect generated by the interpenetrating network prevents ordered arrangement of starch molecular chains, leading to the complete transformation of crystalline structures into amorphous states.

Figures 2(e) and 2(f) display the particle size distribution curves of PAM and IPN-PAM/STA, respectively. Figure 2(e) is the statistical particle size distribution graph of PAM, with an average particle size of 52.15 nm. Its particle size distribution features a sharp peak with a narrow span, demonstrating excellent particle concentration and high uniformity. This indicates that pure polyacrylamide particles

disperse evenly in the system with weak agglomeration effects. Figure 2(f) shows the particle size distribution results of the IPN-PAM/STA composite material, where the average particle size of the sample increases to 85.91 nm. Compared with PAM, the average particle size of the modified system increases significantly, accompanied by a slight broadening of the particle size distribution peak. This indicates that after the introduction of STA monomers and the construction of the IPN interpenetrating network structure, crosslinking entanglement and composite assembly of polymer chains occur, resulting in a remarkable increase in the hydrodynamic size of particles. Nevertheless, the sample still exhibits a regular unimodal distribution without obvious multimodal peaks or micron-scale large agglomerated particles, and severe agglomeration and flocculation are absent. This verifies that the modified IPN-PAM/STA system retains favorable overall dispersion stability.

3.2 Analysis of Swelling Performance

To thoroughly analyze the regulatory mechanism of environmental factors on the stability and swelling behavior of microspheres in this study, the particle size variation rules of microspheres under different salt solutions, pH values and temperatures were systematically investigated, and the specific test results are shown in Figure 3.

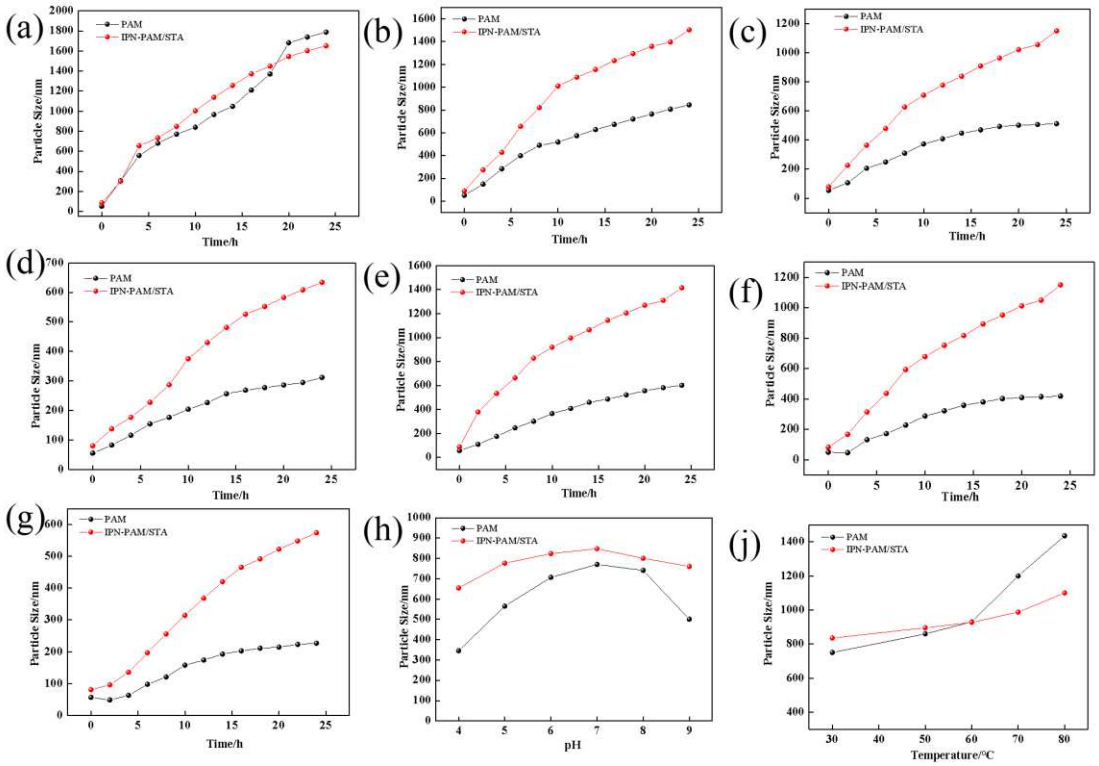


Fig. 3 Swelling performance tests under different conditions: (a) deionized water, (b) 1000 mg/L NaCl solution, (c) 5000 mg/L NaCl solution, (d) 10000 mg/L NaCl solution, (e) 1000 mg/L $CaCl_2$ solution, (f) 5000 mg/L $CaCl_2$ solution, (g) 10000 mg/L $CaCl_2$ solution, (h) solutions with different pH values, (i) temperature

As shown in Figure 3(a), the initial swelling capacity of PAM microspheres in deionized water is significantly superior to that of IPN-PAM/STA microspheres. After the swelling time exceeds 20 h, IPN-PAM/STA microspheres exhibit stronger swelling capacity. This indicates that as IPN-PAM/STA microspheres migrate farther in the formation, they pass through large pores and plug formations with smaller pore sizes, raising the plugging efficiency and further enhancing oil recovery. This solves the problem of low plugging efficiency caused by excessive rapid swelling of microspheres.

Figures 3(b-d) illustrate the effects of NaCl concentration on the swelling performance of PAM microspheres and IPN-PAM/STA microspheres. It can be seen from the figures that under the same NaCl concentration, the initial swelling capacity of PAM microspheres is weaker than that of IPN-PAM/STA microspheres. As NaCl concentration rises, the swelling capacities of both PAM and IPN-PAM/STA

microspheres decrease, yet IPN-PAM/STA microspheres are less affected. Under identical NaCl concentrations, the weaker initial swelling capacity of PAM microspheres mainly stems from the dual-network structure and hydrophobic modification of IPN-PAM/STA microspheres. The interpenetrating network of the latter provides more swelling space, while hydrophobic groups boost water absorption via dynamic crosslinking. The swelling capacity of both microsphere types declines with increasing NaCl concentration, but IPN-PAM/STA microspheres suffer less impact. This is because the synergistic effect of hydrophobic interactions and dual networks effectively counteracts the charge shielding of salt ions on hydrophilic networks and maintains superior structural stability.

In practical oilfield profile control and flooding applications, formation water generally contains high concentrations of Ca^{2+} and Mg^{2+}. Microspheres with insufficient calcium salt resistance will face severe limitations in their application scope. Accordingly, this paper analyzes the influence of $CaCl_2$ on the swelling behavior of microspheres to offer a theoretical basis for the salt-resistant modification design of microspheres. Figures 3(e-g) depict the effects of $CaCl_2$ concentration on the swelling performance of PAM microspheres and IPN-PAM/STA microspheres. The figures reveal that under the same $CaCl_2$ concentration, PAM microspheres possess weaker initial swelling capacity than IPN-PAM/STA microspheres. Rising $CaCl_2$ concentration reduces the swelling capacity of both microspheres, with IPN-PAM/STA microspheres being less affected by the concentration increase, which demonstrates their excellent calcium salt resistance. The dual interpenetrating network structure and hydrophobic modification of IPN-PAM/STA microspheres enable their hydrophobic association and physical crosslinking networks to effectively resist charge shielding and bridging damage exerted by Ca^{2+} on hydrophilic groups, thereby delivering outstanding calcium salt resistance.

Variations in pH alter the dissociation state of ionizable groups (e.g., carboxyl —COOH or amino —NH_2) within the polymer microsphere network, which further impacts electrostatic repulsion and hydrophilicity. For instance, under acidic

conditions, protonation of carboxyl groups (—COO^- → —COOH) weakens intermolecular electrostatic repulsion and lowers the swelling ratio. In alkaline environments, full dissociation of carboxyl groups elevates charge density and strengthens swelling capacity. Additionally, pH may modulate hydrophobic group interactions or crosslinking network stability. To investigate the adaptability of the synthesized microspheres in oilfield profile control and flooding and guarantee stable performance across acidic and alkaline environments, this paper explores the pH effect on the swelling performance of PAM and IPN-PAM/STA microspheres, as presented in Figure 3(h). The figure shows that the swelling capacities of both microspheres first increase and then decline with rising pH, while the swelling variation of IPN-PAM/STA microspheres remains marginal. This phenomenon arises from shifts in the dissociation equilibrium of ionic groups and structural stability within polymer networks. In low-pH ranges, rising pH gradually ionizes carboxyl groups (-COOH) into negatively charged -COO^-, amplifying electrostatic repulsion to expand the network and raise swelling ratios. Swelling reaches its peak under neutral to weakly alkaline conditions. At high pH, excess OH^- not only shields electrostatic repulsion from -COO^- but also triggers amide hydrolysis and network degradation, diminishing swelling capacity. Benefiting from the dual interpenetrating network and hydrophobic association, IPN-PAM/STA microspheres maintain superior stability against pH fluctuations.

Temperature variations drastically modify the mobility of polymer chains, hydrophilic-hydrophobic balance, and intermolecular forces, directly regulating the swelling behavior of microspheres. Elevated temperature accelerates water molecule diffusion and polymer segment motion to facilitate swelling; meanwhile, it may break physical crosslinking points such as hydrogen bonds and hydrophobic interactions, leading to network loosening or disintegration. In high-temperature oil formations, persistent temperature fluctuations impair the long-term stability of microspheres. To validate the practical value of the synthesized microspheres under complex thermal conditions, the temperature dependence of swelling performance is studied, as shown in Figure 3(i). The figure indicates that the swelling capacities of PAM and

IPN-PAM/STA microspheres both rise with increasing temperature. At temperatures below 60 ℃, PAM microspheres exhibit weaker swelling capacity than IPN-PAM/STA microspheres. When temperatures exceed 60 ℃, PAM microspheres display stronger swelling capacity, and dissolution of PAM microspheres occurs above 70 ℃ At low temperatures, the physical crosslinking network formed by the dual interpenetrating structure and hydrophobic association endows IPN-PAM/STA microspheres with better swelling performance than single-network PAM microspheres. As temperature climbs, increased thermal energy weakens hydrophobic association and contracts the IPN-PAM/STA network, whereas intensified thermal motion of PAM molecular chains boosts swelling and surpasses the swelling capacity of IPN-PAM/STA microspheres. Above 70 ℃, PAM microspheres dissolve due to crosslinking network breakdown, while IPN-PAM/STA microspheres retain structural integrity via the synergistic combination of chemical crosslinking and interpenetrating networks. This confirms that the IPN-PAM/STA microspheres synthesized in this work feature favorable temperature resistance.

3.3 Evaluation of Core Sealing Performance

As shown in Figure 4, the saturated artificial core was first treated with distilled water for displacement. When pressure gradually stabilized, IPN-PAM/STA microsphere aqueous solution was introduced for displacement, and pressure changes were monitored. With increasing time, the pressure rose progressively, indicating migration of IPN-PAM/STA microspheres within the core; the subsequent pressure increase confirmed their effective sealing action. During a sudden pressure drop, the microspheres had migrated to the opposite end of the core. Continued displacement with distilled water resulted in further pressure elevation, demonstrating complete sealing. Post-sealing analysis of the injection profile revealed yellowish zones throughout the profile with no visible gelation, confirming successful microsphere penetration. This phenomenon demonstrates that under suitable conditions, microspheres can migrate deep into the formation to achieve depth-dependent profile modification. Calculations show: initial permeability with distilled water injection

was 0.95 mD; permeability after 0.5% microsphere injection was 0.03 mD, yielding a sealing efficiency of 96.3%; final permeability with distilled water injection dropped to 0.02 mD—significantly higher than conventional microspheres' 72%. These results indicate substantial improvements in both microsphere strength and expansion performance.

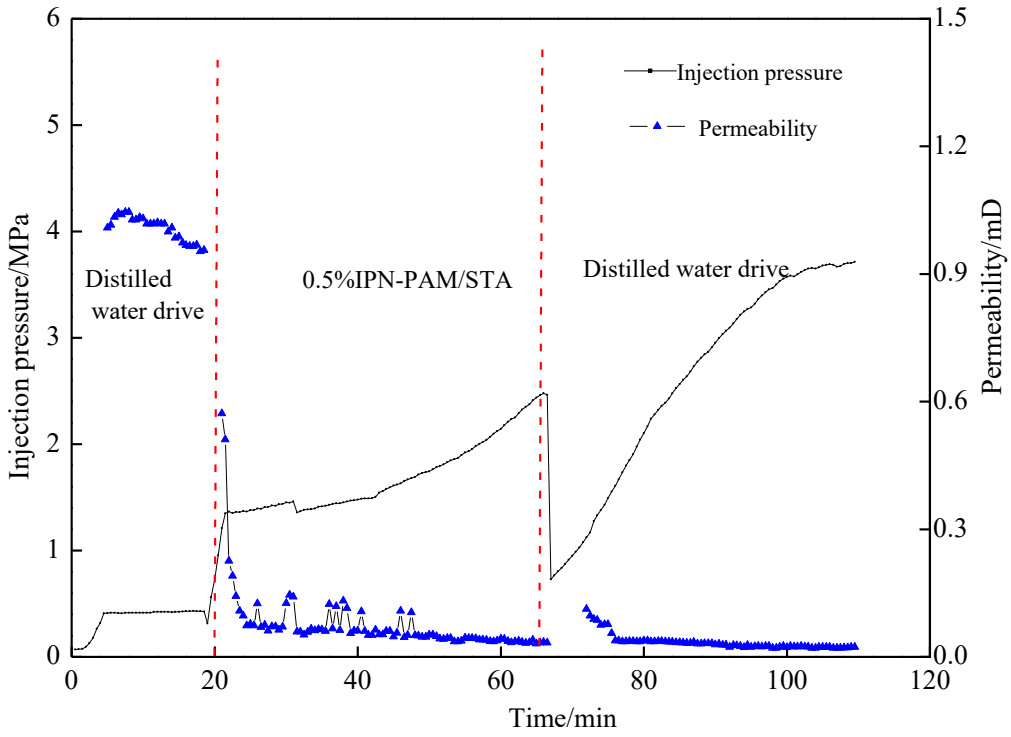


Figure 4 Schematic diagram of the occlusion experiment using IPN-PAM/STA microsphere modulators

3.4 Analysis of the Sealing Mechanism

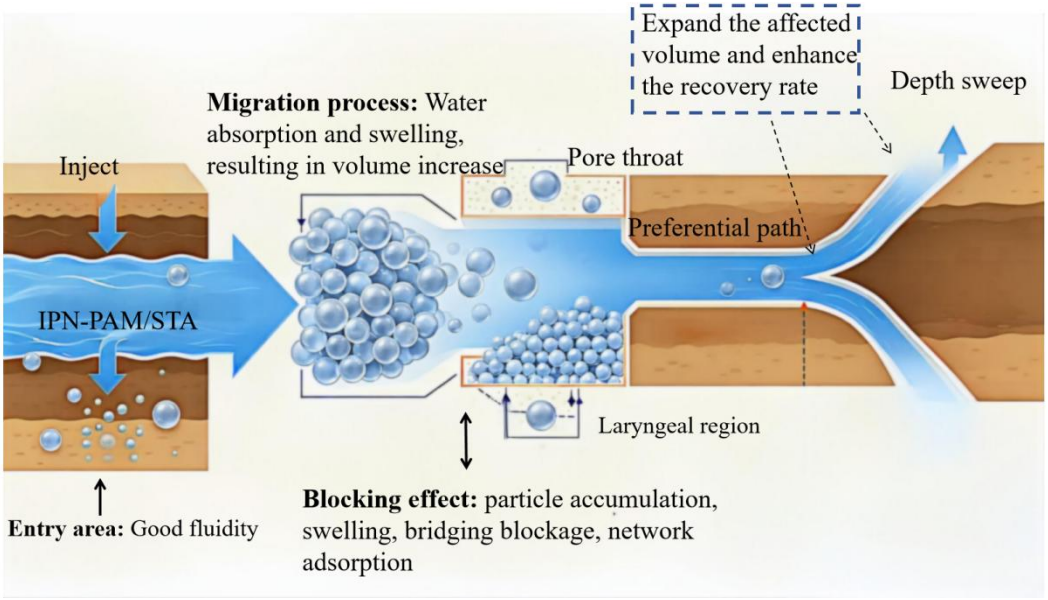


Fig. 5 Plugging Mechanism of IPN-PAM/STA

Figure 5 illustrates the plugging mechanism of IPN-PAM/STA. As shown, after the microsphere dispersion system is injected into the formation, it initially maintains good fluidity in the near-well zone; subsequently, during migration, it gradually absorbs water and swells, increasing its volume and enhancing its pore-plugging capacity; upon reaching deeper layers, the microspheres reduce permeability in high-permeability zones through particle accumulation, swelling, bridging effects, and network adsorption, forcing subsequent injection water to flow into previously unaffected areas, thereby expanding the effective sweep volume and improving oil recovery. Therefore, the occlusion mechanism of IPN-PAM/STA microspheres results from the combined effects of a cross-linked network structure, moderate swelling, deep migration, pore-throat bridging, temperature and salt resistance, and biodegradability.

3.5 Analysis of Biodegradation Performance

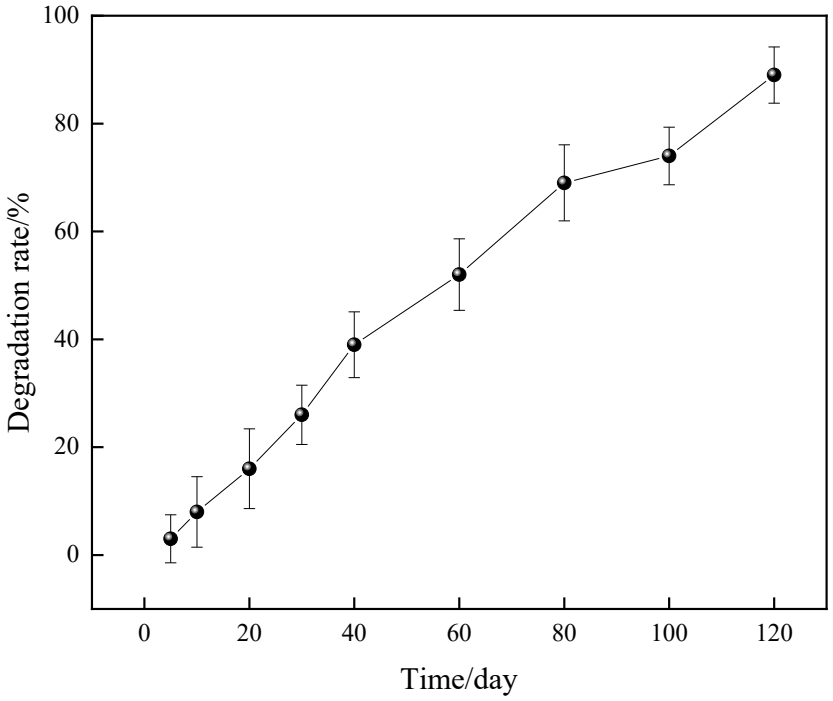


Fig. 6 Degradation rates of IPN-PAM/STA at different time points

Water-soluble starch is a natural, renewable material that can be effectively degraded when buried in soil due to the abundance of microorganisms in the environment. Figure 6 shows the degradation rate of IPN-PAM/STA microsphere samples embedded in garden soil at a depth of 20 cm over 120 days. The data indicate that the biodegradation rate of IPN-PAM/STA microspheres increased steadily over time: the degradation rate was rapid during the first 40 days; although it slowed thereafter, the rate continued to rise steadily, reaching over 90% by day 120. This demonstrates that IPN-PAM/STA microspheres pose no secondary environmental pollution and represent a viable environmentally friendly sealing material.

4 Conclusion

This study successfully prepared IPN-PAM/STA interpenetrating network microspheres using acrylamide (AM) as the first network and acid-treated starch (STA) as the second network through inverse-phase emulsion polymerization, establishing optimal preparation conditions and completing structural characterization. FT-IR and XRD analyses confirmed that starch and PAM form a stable interpenetrating network

structure, where starch hydroxyl groups establish strong hydrogen bonds with PAM amide groups, disrupting the original crystalline structure of starch into an amorphous state. TGA and DSC tests demonstrated that these microspheres exhibit significantly superior thermal stability compared to conventional PAM microspheres, with lower weight loss above 400°C and maintained structural integrity beyond 70°C, demonstrating excellent high-temperature adaptability. The IPN-PAM/STA microspheres demonstrate outstanding comprehensive performance, effectively addressing the limitations of traditional PAM microspheres: controllable swelling rates, superior swelling capacity after 20 hours, excellent salt resistance (particularly against calcium salts), good tolerance to pH fluctuations, and exceptional stability in complex reservoir environments. Core plugging experiments showed a plugging efficiency of 96.3%, far exceeding the 72% of conventional microspheres, enabling effective profile modification and water blocking in deep formations. Biodegradation tests revealed over 90% degradation rate within 120 days, confirming their status as environmentally friendly materials. In summary, IPN-PAM/STA microspheres meet the demands of profile modification and water blocking in complex reservoirs, providing a novel, efficient, and eco-friendly solution for enhancing crude oil recovery rates.

Statements and Declarations

CRediT authorship contribution statement

Guangliang Jia: Conceptualization, Funding Acquisition; **Guiru Liu:** Conceptualization, Methodology, SoftwareInvestigation, Formal Analysis, Writing - Original Draft, **Xin Wen:** Writing - Review & Editing; **Daoming Zheng:** Conceptualization, Funding Acquisition; **Yunchao Chang:** Supervision, Visualization.

Declaration of Competing Interest

The authors declare that they have no known competing financial interests or personal relationships that could have appeared to influence the work reported in this paper.

Acknowledgements

This research was financially supported by Sinopec Petroleum Engineering Technology Service Company Project Research on Fracturing Techniques and

High-Efficiency Gas Recovery Methods for Deep Coalbed Methane Reservoirs in the Ordos Basin(SG2402-03K), The Postdoctoral Scientific Research Project of Shaanxi Province (Grant No.2025BSHSDZZ341), Shaanxi Province Youth Fund(2025JC-YBQN-886).

References

[1]Song ZJ, Hou JG, Lai XJ, et al. Preparation and Performance Evaluation of Novel Interpenetrating Network Microsphere Modulating and Dissolving Agents[J]. Modern Chemical Industry, 2022, 42(4): 173-181.

[2]Hou JR, Chen YG, Wu Y, et al. Microscopic oil displacement characteristics of polymer surfactant solutions[J]. Oilfield Chemistry, 2020, 37(2): 292-296.

[3]]Zhang YS, Liu Q,Peng B, Luo D. Development of smart nanoparticles for enhanced oil recovery[J]. Modern Chemical Industry, 2020, 40(6): 1-6.

[4] Qu Haiying,Liu Qi,Peng Bo, et al. Effect of nanoparticle on stability of CO2 foam flooding sys-tem[J]. Petroleum Geology and Recovery Efficiency,2019,26(5): 1-7.

[5] Zhang Q, Li G, Fu ML, Zuo JQ, et al. Research Progress on Water Loss of Polymer Gel for Water Blocking [J]. Applied Chemical Engineering, 2019, 48(4): 970-974.

[6] Wu TJ, Zheng MK, Zhou ZP. New method for plugging performance evaluation of polymeric nanospheres in low permeability reservoir[J]. Fault-Block Oil & Gas Field, 2018, 25(4): 498- 501.

[7] Zhou W, Xin C, Chen Y, et al. Nanoparticles for enhancing heavy oil recovery: recent progress, challenges, and future perspectives[J]. Energy & Fuels, 2023, 37(12): 8057-8078.

[8] Lin M, Zhao Q, Dang S. Preparation and properties of terpolymeric microspheres for deep profile control in oilfields[J]. Material Research Innovations, 2016, 19(5): 574-579.

[9] Wang Z, Zhao X, Bai Y. Study of a double cross-linked HPAM gel for in-depth profile control[J]. Journal of Dispersion Science and Technology,2016,37(7) : 1010-1018.

[10] Liu Y, Ma JZ, Yang H, Cao RR, et al. Preparation of Polyacrylamide Microspheres by Reverse Emulsion Method and Their Properties Research [J]. Daily Chemical Industry, 2020,50(4):238-243.

[11] Liu XF, Qi PY, Cheng C, et al. Study on Rheological and Swelling Properties of Nano-Polyacrylamide Microspheres [J]. Journal of Tianjin University, 2021, 54(9): 950-955.

[12] Dong LG. Synthesis of Polyacrylamide by Reverse Emulsion Polymerization [J]. Applied Chemical Engineering, 2011,40(6):1029-1031.

[13] Lu Y, Kang WL, Wai R. Research progress on acrylamide based polymer fracturing fluid[J]. Polymer Materials Science and Engineering, 2018, 34(12): 161-167.

[14] Wen X, Fei GQ, Liu GR, et al. Study on Preparation of Degradable Hydrogels Based on Novel Castor Oil-Derived Crosslinker MCOA and Their Adsorption Mechanism for Cu^{2+} and Pb^{2+}[J]. Colloids and Surfaces A: Physicochemical and Engineering Aspects, 2025: 139399.